Space charge limited photoelectric emission in a plane parallel electrode geometry

1972 J. Phys. A: Gen. Phys. 5 1337

(http://iopscience.iop.org/0022-3689/5/9/007)

J. Phys. A: Gen. Phys., Vol. 5, September 1972. Printed in Great Britain.

Space charge limited photoelectric emission in a plane parallel electrode geometry

C B WHEELER

Plasma Physics Department, Imperial College, London SW7, UK

MS received 23 March 1972

Abstract. The problem of space charge limited photoelectric emission in a plane parallel electrode geometry is considered for an emitting electrode composed of material with a constant optical absorption coefficient and a classical step surface barrier. Poisson's equation is solved for the limit of zero cathode temperature and this solution shown to be applicable to the general case if the ratio of the collection current J to the saturation current J_s satisfies $(\pi^2/3)\{kT/h(\nu-\nu_0)\}^2 \ll J/J_s \leqslant 0{\cdot}5$ where T is the cathode temperature, $h\nu$ the incident quantum energy and $h\nu_0$ the threshold energy. For a given anode voltage of either polarity it is shown that there are three characteristic anode currents—the current for onset of space charge limitation, the maximum limited current and the completely limited current. When the anode is positive all three currents are greater than the Langmuir–Child limit. For zero anode voltage the current flow is always space charge limited and also exhibits a maximum and complete limitation. When limitation takes place the space charge potential minimum is always situated between the cathode and the midelectrode plane if the anode is positive, whereas for a negative anode it can be positioned anywhere between the electrodes.

1. Introduction

The influence of space charge on the process of thermionic emission in a plane parallel electrode geometry was first considered by Fry (1921) and subsequently extended by Langmuir (1923). This paper is concerned with the additional process of photoelectric emission, thereby introducing two more variables into the analysis, namely the intensity and frequency of the radiation illuminating the emitting electrode. In order that the problem can be tackled analytically it is necessary to restrict considerations to pure metal cathodes for which a very simple model of the emission process is valid, as shown by the pioneer work of Fowler (1931) and Dubridge (1933). Consequently the results of this present work are only rigorously applicable to systems using pure metal cathodes such as the gold or palladium photocathodes that are used in demountable systems. However the results can be tentatively applied to more complex cathode materials if operation is carried out very near to the threshold region. Such operation ensures that the electron emission spectrum is largely determined by the well defined tail of the energy distribution of electrons within the cathode material. The formulation of the general space charge problem follows closely the treatment given by Fry (1921) and all quantities are expressed in the CGS ESU system.

2. General mathematical formulation

Consider a plane parallel electrode configuration situated in vacuum and let the cathode emit a steady stream of electrons of unspecified energy distribution. If the anode is at

a positive potential and does not collect the full saturation current then there must be a region of negative potential gradient adjacent to the cathode, produced by space charge, that repels some of the emitted electrons back to the cathode. Let x denote the position and V the potential of a point in the electron cloud, both measured relative to the cathode. In particular let x_m, V_m denote these quantities for the potential minimum between the electrodes. If space charge limitation of the current is taking place then V_m must exist and be a negative quantity. It is convenient to define the electron energy distribution at the cathode in terms of the normal velocity u such that $n(u)\,du$ is the number of electrons emitted per second per unit area of cathode with normal velocity components in the interval u, du. The saturation current density is therefore

$$J_s = e\int_0^\infty n(u)\,du \tag{1}$$

where e is the magnitude of the electronic charge. The current density collected at the anode, when space charge limitation is taking place, is determined by the number of electrons that can pass the potential minimum V_m

$$J = e\int_{u_m}^\infty n(u)\,du \tag{2}$$

with

$$\tfrac{1}{2}mu_m^2 = -eV_m \tag{3}$$

where m is the electronic mass. At any position x the electron velocity v at that point is related to the emission velocity u and local potential V through

$$\tfrac{1}{2}mv^2 = \tfrac{1}{2}mu^2 + eV. \tag{4}$$

Let the interelectrode space be divided into two regions; the anode region $x_m \leqslant x \leqslant x_a$ and the cathode region $0 \leqslant x \leqslant x_m$ where x_a is the electrode separation. In each of these regions the space charge density is obtained by dividing the number of electrons passing through unit area per second by their local velocity. For the anode region this density is therefore

$$\rho = -e\int_{u_m}^\infty \frac{n(u)}{v}\,du \qquad x_m \leqslant x \leqslant x_a. \tag{5}$$

In the cathode region the electrons at any point can be divided into two categories. There are those electrons entering into equations (2) and (5) that proceed past the potential minimum to the anode, and those of lower energy that can reach the relevant position x but are subsequently turned back again by the prevailing negative potential gradient. This latter category is therefore composed of two equally dense electron streams moving in opposite directions. The space charge density in this cathode region is then

$$\rho = -e\int_{u_m}^\infty \frac{n(u)}{v}\,du - 2e\int_{u_x}^{u_m} \frac{n(u)}{v}\,du \qquad 0 \leqslant x \leqslant x_m \tag{6}$$

with

$$\tfrac{1}{2}mu_x^2 = -eV. \tag{7}$$

The charge densities of equations (5) and (6) must be related to the potentials contained

implicitly within them through Poisson's equation

$$\frac{d^2V}{dx^2} = -4\pi\rho.$$

Multiply both sides of Poisson's equation by $2dV/dx$ where, from equation (4) $2\,dV/dx = (2mv/e)\,dv/dx$, and substitute for the charge density from equation (6). With these operations Poisson's equation in the cathode region becomes

$$\frac{d}{dx}\left(\frac{dV}{dx}\right)^2 = 8\pi m\left(\int_{u_m}^{\infty} n(u)\,du\,\frac{dv}{dx} + 2\int_{u_x}^{u_m} n(u)\,du\,\frac{dv}{dx}\right) \qquad 0 \leqslant x \leqslant x_m.$$

Integrate both sides with respect to x remembering that the integration limit $dV/dx = 0$ corresponds to $V = V_m$ and therefore to $x = x_m$. In the case of the second integral, where u_x is a function of x, the integrand is zero at $x = x_m$ since at this position $u_x = u_m$. This first integration leads to

$$\left(\frac{dV}{dx}\right)^2 = 8\pi m\left(\int_{u_m}^{\infty} (v-w)n(u)\,du + 2\int_{u_x}^{u_m} vn(u)\,du\right) \qquad 0 \leqslant x \leqslant x_m$$

with

$$\tfrac{1}{2}mw^2 = \tfrac{1}{2}mu^2 + eV_m \tag{8}$$

where w is the electron velocity evaluated at the position $x = x_m$. The corresponding expression for the anode region, $x_m \leqslant x \leqslant x_a$, is simply the above expression with the omission of the final integral. At this point in the analysis Fry (1921) introduced the maxwellian distribution for $n(u)$ to represent thermionic emission from the cathode. However the analysis can be pursued further, as follows, without specifying the form of the electron emission spectrum. By suitable division of the integration limits the following expression can be formulated, applicable to both the interelectrode regions

$$\frac{1}{8\pi m}\left(\frac{dV}{dx}\right)^2 = \int_{u_x}^{\infty} vn(u)\,du \pm \int_{u_x}^{u_m} vn(u)\,du - \int_{u_m}^{\infty} wn(u)\,du$$

where the positive sign is applicable to the cathode region and the negative sign to the anode region. The integration limits in this equation can be simplified by expressing each integral completely in terms of one particular velocity variable. Express the first two integrals entirely in terms of the velocity v with distribution $n(v)$ such that $n(v)\,dv = n(u)\,du$ where $v = 0$ at $u = u_x$; and express the final integral in terms of the velocity w with distribution $n(w)\,dw = n(u)\,du$ where $w = 0$ at $u = u_m$. Then

$$\frac{1}{8\pi m}\left(\frac{dV}{dx}\right)^2 = \int_0^{\infty} vn(v)\,dv \pm \int_0^{v_m} vn(v)\,dv - \int_0^{\infty} wn(w)\,dw \tag{9}$$

where, from equations (3) and (4)

$$\tfrac{1}{2}mv_m^2 = e(V - V_m). \tag{10}$$

The integrals on the right of equation (9) must be evaluated before a second integration with respect to x can be carried out, this requires a knowledge of the velocity distribution function. Fowler (1931) made the first successful attempt at calculating the normal velocity spectrum of photoelectrons emitted from a hot plane cathode of pure metal illuminated by monochromatic radiation. His treatment was based on the following three simple assumptions. Firstly within the photocathode material the number of

electrons passing through unit area per second with velocity components normal to the surface in the interval ω, $d\omega$ is given by Fermi–Dirac statistics as

$$n(\omega)\,d\omega = 4\pi m^2 \frac{kT}{h^3}\omega \ln\left\{1+\exp\left(\frac{E-\frac{1}{2}m\omega^2}{kT}\right)\right\} d\omega \tag{11}$$

where E is the greatest electron energy at absolute zero and T the cathode temperature. Secondly it is assumed that the probability of an electron in the metal absorbing a quantum is proportional to the intensity of the illumination and that the absorbed quantum contributes only to the electron energy normal to the cathode surface. The final assumption is that the electron travels without energy loss to the surface of the cathode where the transmission coefficient is unity if the total normal energy of the electron exceeds some critical value W and equal to zero for energies less than this value. These latter two assumptions infer that the normal velocity of emission u is related to the velocity ω inside the metal and to the illuminating quantum energy $h\nu$ through

$$\tfrac{1}{2}mu^2 = \tfrac{1}{2}m\omega^2 + h\nu - W. \tag{12}$$

Substitution of equation (12) into (11) gives the required normal emission spectrum

$$n(u)\,du = 4\pi AIm^2 \frac{kT}{h^3} u \ln\left\{1+\exp\left(\frac{h(\nu-\nu_0)-\frac{1}{2}mu^2}{kT}\right)\right\} du \tag{13}$$

where $h\nu_0 = W - E$ is the threshold energy, I the intensity of photocathode illumination and A a constant dependent on the nature of the cathode material.

3. The low frequency approximation

The space charge problem in thermionic emission is a special case of the above general formulation. Equation (13) shows that pure thermionic emission takes place when the illuminating frequency ν approaches zero. The exponential term is then small in magnitude and the logarithm can be expanded to first order. This results in the maxwellian distribution that was inherently assumed by the early workers in this field. Substitution of this distribution into equation (1) leads to the Dushman equation of thermionic emission with the cathode work function reduced by the quantum energy $h\nu$. Equations (1) and (2) together give

$$J/J_s = \exp\left(\frac{eV_m}{kT}\right). \tag{14}$$

Substitution of the maxwellian distribution into equation (9) and evaluation of the exponential integrals leads to the differential equation given by Langmuir (1923). The result is quoted below for the purposes of comparison with later expressions

$$\left(\frac{d\eta}{d\xi}\right)^2 = \exp(\eta) \pm \{\exp(\eta)\,\mathrm{erf}(\eta^{1/2}) - 2\pi^{-1/2}\eta^{1/2}\} - 1 \tag{15}$$

where

$$\eta = e\frac{(V-V_m)}{kT} \tag{16}$$

and

$$\xi = 4(\tfrac{1}{2}\pi)^{3/4} m^{1/4} e^{1/2} J_s^{1/2} (kT)^{-3/4} (x - x_m). \tag{17}$$

In principle equations (14), (15), (16) and (17) enable complete solution of the space charge problem in thermionic emission.

4. The low temperature approximation

At temperatures near absolute zero equation (13) shows that electron emission is only possible if $v > v_0$. In this case the factor of unity can be neglected in comparison with the large exponential term. The resulting distribution is independent of temperature and is cubic in velocity with a cut off at the value given by the Einstein relation $\frac{1}{2}mu^2 = h(v - v_0)$. Equations (1) and (2) now give

$$\frac{J}{J_s} = \left(1 + \frac{eV_m}{h(v - v_0)}\right)^2. \tag{18}$$

Evaluation of the simple integrals that occur in equation (9) leads to

$$\left(\frac{d\alpha}{d\beta}\right)^2 = 2(\alpha + 1)^{5/2} \pm \alpha^{3/2}(2\alpha + 5) - 2 \tag{19}$$

where

$$\alpha = \left(\frac{J_s}{J}\right)^{1/2} \frac{e(V - V_m)}{h(v - v_0)} \tag{20}$$

and

$$\beta = 4\left(\frac{2\pi\sqrt{2}}{15}\right)^{1/2} m^{1/4} e^{1/2} \left(\frac{J}{J_s}\right)^{1/8} J_s^{1/2} \{h(v - v_0)\}^{-3/4} (x - x_m). \tag{21}$$

Comparison of these last three equations with equations (15), (16) and (17) shows the broad qualitative difference expected from physical considerations, namely the replacement of the thermal energy kT by the energy quantum $h(v - v_0)$. Before resorting to numerical integration of equation (19) it is convenient to consider the general case of arbitrary frequency and temperature.

5. The general case

Substitution of equation (13) into equations (1) and (2) produces integrations of the type already performed by Fowler (1931) and leads to

$$J_s = 4\pi A I e m \frac{(kT)^2}{h^3} \left(\frac{\pi^2}{6} + \frac{\gamma^2}{2} + \sum_1^\infty (-1)^n n^{-2} \exp(-n\gamma)\right) \tag{22}$$

where

$$\gamma = \frac{h(v - v_0)}{kT} \tag{23}$$

$$J = 4\pi A I e m \frac{(kT)^2}{h^3} \left(\frac{\pi^2}{6} + \frac{\delta^2}{2} + \sum_1^\infty (-1)^n n^{-2} \exp(-n\delta)\right) \tag{24}$$

where

$$\delta = \frac{h(\nu - \nu_0) + eV_m}{kT}. \tag{25}$$

Equation (22) forms the basis of the Fowler (1931) technique for measurement of threshold energy in which an experimental plot of $\lg(J_s/T^2)$ against $h\nu/kT$ is made and the displacement of this curve from the above theoretical curve determined. Equation (24) forms the basis of the Dubridge (1933) technique in which $\lg(J/T^2)$ is plotted against eV_m/kT where, in this case, V_m is the negative potential of the retarding anode and space charge limitation is assumed to be negligible. The results obtained by Dubridge are particularly relevant to the problem in hand that is concerned with the flow of electrons from a photocathode past a potential barrier produced by space charge rather than by a retarding anode. By differentiation of his experimental current–voltage characteristic he obtained the electron velocity distribution and compared it with equation (13). There was excellent agreement for the high velocity portion of the distribution that constituted half of the saturation current but there was a notable deficiency of low velocity electrons in comparison with the theoretical expression. Dubridge correctly attributed this discrepancy to theoretical oversimplification of the optical absorption coefficient and surface transmission coefficient. Both of these parameters are functions of the electron velocity within the metal but their dependence is weak in comparison with that of the dominant tail of the Fermi–Durac distribution, hence their valid approximation to a constant for the high velocity portion of the spectrum. The theoretical overestimate to the number of slow electrons will, from equations (5) and (6), lead to overestimation of the space charge density and its associated potential minimum. Consequently the following calculations, which are based on equation (13), will lead to an underestimate in the value of J, particularly in the region where $0{\cdot}5 \leqslant J/J_s \leqslant 1$.

Substitution of equation (13) into equation (9) results in integrations that cannot be performed exactly analytically. In the appendix these integrations are evaluated in the form of power series in the dimensionless parameters δ and ϵ where

$$\epsilon = \frac{h(\nu - \nu_0) + eV}{kT}. \tag{26}$$

Equation (9) is then expressible as

$$\begin{aligned}\frac{h^3}{32\sqrt{(2)}\pi^2 AIm^{3/2}(kT)^{5/2}}\left(\frac{dV}{dx}\right)^2 &= \frac{4}{15}\epsilon^{5/2} \pm \frac{2}{15}(\epsilon-\delta)^{3/2}(2\epsilon+3\delta) - \frac{4}{15}\delta^{5/2} + \frac{\pi^2}{6}(\epsilon^{1/2}-\delta^{1/2}) - \frac{7\pi^4}{1440}(\epsilon^{-3/2}-\delta^{-3/2}) \\ &\quad + O[\epsilon^{-7/2}, \delta^{-7/2}, \epsilon^{1/2}\exp(-\epsilon), \delta^{1/2}\exp(-\delta), \\ &\quad (\epsilon-\delta)^{1/2}(\exp(-\delta)-\exp(-\epsilon))].\end{aligned} \tag{27}$$

Since V_m is the potential minimum, it follows from equations (25) and (26) that $\epsilon \geqslant \delta$. Consequently the above power series converges rapidly for sufficiently large values of δ. If only the 5/2 power terms need be retained then equation (27) becomes independent of temperature and reduces identically to the low temperature approximation of equation (19). Under the same condition, since $\gamma \geqslant \delta$, equations (22) and (24) reduce identically to equation (18). A closer examination of the convergence of equation (27), which is

least rapid for the negative sign and for $\epsilon \gg \delta$, shows that the 5/2 power terms exceed all other terms if $\delta^2 > \pi^2/3$. This convergence condition, in conjunction with equation (18), defines a lower limit to the parameter J/J_s:

$$J/J_s \gg \frac{\pi^2}{3}\left(\frac{kT}{h(\nu-\nu_0)}\right)^2.$$

Physically this condition implies that the bulk of the electrons that overcome the potential minimum must do so with excess energies of many times the thermal energy. In practical terms this condition is not severely restrictive since most photoelectric devices are operated at room temperature or reduced temperature. For example at room temperature with a threshold of $h\nu_0 = 5\,\text{eV}$ (2500 Å wavelength) the inequality requires $J/J_s \gg 2\times10^{-3}$ for a photon energy of $h\nu = 6\,\text{eV}$ (2000 Å).

The foregoing discussion and calculation indicates that the low temperature approximation of the previous section correctly describes the general problem provided the parameter J/J_s is confined between the following limits

$$\frac{\pi^2}{3}\left(\frac{kT}{h(\nu-\nu_0)}\right)^2 \ll \frac{J}{J_s} \leqslant 0{\cdot}5. \tag{28}$$

Table 1 gives the numerical solution to equation (19) evaluated to 4 significant figures and figure 1 shows the general behaviour of the parameters α and β. The negative values of β correspond to the cathode region $0 \leqslant x \leqslant x_m$ and the positive values to the anode region $x_m \leqslant x \leqslant x_a$. In the cathode region β asymptotically approaches the value of 2·396 and there is an analogous behaviour for the thermionic parameters η and ξ in equation (15) where ξ has the asymptotic value of 2·554. The following limiting series solutions are useful.

Anode region

$$\begin{aligned} &\alpha \gg 1 \qquad \beta = \frac{8}{3\sqrt{(15)}}(\alpha^{3/4}+\tfrac{4}{5}\alpha^{1/4}-O(\alpha^{-1/4}))-0{\cdot}093 \\ &\alpha \ll 1 \qquad \beta = \frac{2}{\sqrt{5}}(\alpha^{1/2}+\tfrac{1}{4}\alpha-O(\alpha^2)). \end{aligned} \tag{29}$$

Cathode region

$$\begin{aligned} &\alpha \gg 1 \qquad \beta = -2{\cdot}396+2\alpha^{-1/4}-\tfrac{1}{2}\alpha^{-5/4}+O(\alpha^{-9/4}) \\ &\alpha \ll 1 \qquad \beta = -\frac{2}{\sqrt{5}}\{\alpha^{1/2}-\tfrac{1}{4}\alpha+O(\alpha^2)\}. \end{aligned} \tag{30}$$

6. Restricted areas in the current–voltage plane

The boundary conditions used in §2 for the first integration of Poisson's equation assume the existence of a potential minimum between the anode and cathode. This existence requires that x_m satisfies the relation $0 \leqslant x_m \leqslant x_a$ and it follows that certain areas in the anode current–voltage plane can be defined where space charge limitation of the anode current takes place.

The lower limit, $x_m = 0$, requires that $V_m = 0$, corresponding to zero field at the cathode and the minimum can only be situated there if the anode potential V_a is positive.

Table 1. Numerical solution to equation (19). β is positive in the anode region and negative in the cathode region.

α	$-\beta$	$+\beta$	α	$-\beta$	$+\beta$
0·00	0·0000	0·0000	8·2	1·247	4·150
0·05	0·1888	0·2112	9·0	1·271	4·413
0·1	0·2606	0·3051	10·6	1·312	4·921
0·2	0·3558	0·4443	12·2	1·347	5·407
0·3	0·4240	0·5562	13·8	1·376	5·875
0·4	0·4783	0·6538	15·4	1·402	6·328
0·5	0·5239	0·7422	17·0	1·425	6·768
0·6	0·5632	0·8241	20	1·462	7·562
0·7	0·5980	0·9010	25	1·511	8·816
0·8	0·6291	0·9739	30	1·549	10·00
0·9	0·6574	1·044	35	1·580	11·14
1·0	0·6832	1·111	40	1·606	12·23
1·2	0·7291	1·238	45	1·628	13·28
1·4	0·7689	1·358	50	1·648	14·30
1·6	0·8040	1·472	60	1·681	16·27
1·8	0·8354	1·582	70	1·707	18·15
2·0	0·8638	1·687	80	1·730	19·96
2·2	0·8897	1·789	90	1·749	21·71
2·4	0·9134	1·888	100	1·765	23·41
2·6	0·9353	1·984	200	1·865	38·58
2·8	0·9557	2·079	300	1·916	51·82
3·0	0·9746	2·170	400	1·949	63·94
3·4	1·010	2·349	500	1·974	75·31
3.8	1·043	2·520	600	1·992	86·09
4·2	1·069	2·686	700	2·008	96·43
4·6	1·096	2·847	800	2·020	106·4
5·0	1·116	3·004	900	2·031	116·1
5·8	1·156	3·307	1000	2·041	125·4
6·6	1·190	3·598	—	—	—
7·4	1·220	3·878	∞	2·396	∞

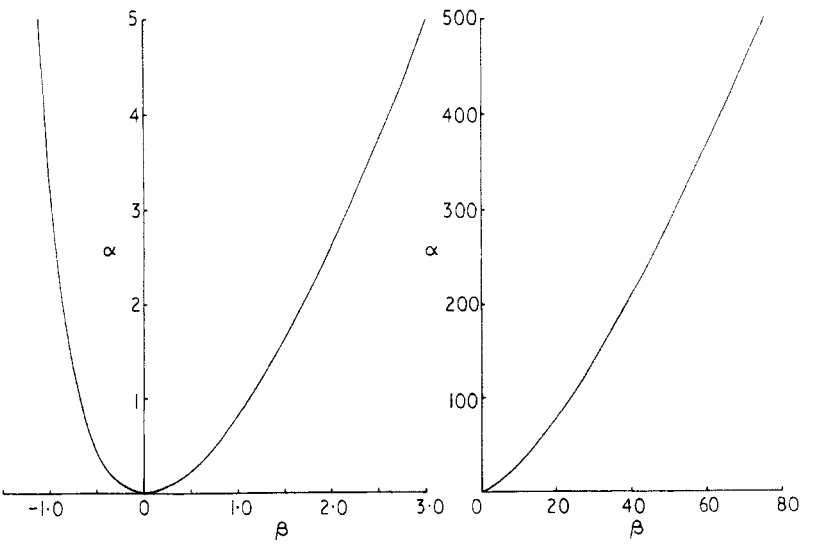

Figure 1. Dependence of α on β according to table 1.

For $V_m = 0$ equation (18) requires that $J/J_s = 1$. It is convenient to express the saturation and anode currents in terms of the current density J_1 where

$$J_1 = (9\pi)^{-1}\left(\frac{2e}{m}\right)^{1/2}\left(\frac{h(\nu-\nu_0)}{e}\right)^{3/2} x_a^{-2}. \tag{31}$$

The current–voltage relation defining this limit can be evaluated from equations (20) and (21) in conjunction with table 1 and the first quadrant in figure 2(*a*) shows the results for anode voltages such that $0 \leqslant eV_a/h(\nu-\nu_0) \leqslant 1$. Figure 2(*b*) shows the results for greater anode voltages, presented logarithmically, with currents expressed in terms of the voltage dependent current density J_v where

$$J_v = (9\pi)^{-1}\left(\frac{2e}{m}\right)^{1/2} V_a^{3/2} x_a^{-2}. \tag{32}$$

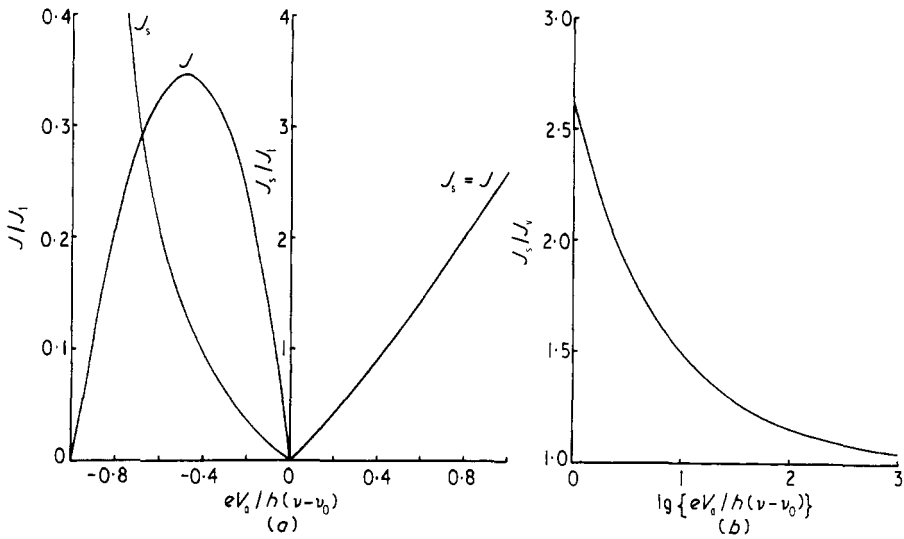

Figure 2. Space charge limited regions in the anode current–voltage plane. (*a*) Small anode voltages, currents expressed in terms of J_1. (*b*) Large positive anode voltages, currents expressed in terms of J_v.

This current density is the space charge limit derived by Langmuir (1913) and Child (1911) under the same conditions of zero field at the cathode but with the simplifying assumption of zero velocity of electron emission. The departure of the ordinates from unity on this curve is therefore a direct consequence of finite velocities of emission. Comparison of equations (31) and (32) shows that J_1 is the value of J_v corresponding to $eV_a/h(\nu-\nu_0) = 1$. The region lying below these two curves for positive anode voltages corresponds to $x_m \leqslant 0$, indicating that there is no potential minimum between the electrodes. Consequently all the electrons emitted from the cathode are collected by the anode and $J/J_s = 1$ throughout this region. The region lying above the curves corresponds to $0 < x_m < x_a$, indicating the existence of a potential minimum and therefore requiring $J/J_s < 1$.

The upper limit, $x_m = x_a$, requires that $V_m = V_a$, corresponding to zero electric field at the anode and a negative anode voltage. This negative voltage requires that

$J/J_s < 1$ since velocities of electron emission down to zero are present, but this does not necessarily mean that the anode current is limited by space charge effects. The second quandrant in figure 2(*a*) shows the individual curves for J_s and J that define this limit. There is space charge limitation of the current in the region above the curves, corresponding to $0 < x_m < x_a$. The region below the curves corresponds to $x_m > x_a$, indicating the absence of such limitation. However in this lower region the anode current is completely determined by the number of electrons with sufficient energy to overcome the negative potential of the anode. This current is given by equation (18) with V_m replaced by V_a. The current density J drops to zero as $eV_a/h(\nu - \nu_0) \to -1$, but the cut off is only sharp for a cathode temperature of absolute zero otherwise the calculations are not valid in this region, as indicated by equation (28). The case of $V_a = 0$ is a singular point since the two curves for $x_m = x_a$ and $x_m = 0$ with the requirement that $J = J_s = 0$. This implies that the interelectrode space is then a region of constant zero potential and if any current is caused to flow at $V_a = 0$ then it must be space charge limited. The maximum in J in the second quadrant shows that a current density of $J > 0{\cdot}35J_1$ cannot be collected by a negative anode without space charge limitation taking place.

7. The approach to complete space charge limitation

In the case of large positive anode voltages equation (29) evaluated at the anode enables J to be expressed in terms of J_s, $eV_a/h(\nu - \nu_0)$, x_a and x_m. The parameter x_m can be determined from equation (30) evaluated at the cathode and the net result is the following expression for J, valid for all $J_s/J \geqslant 1$ and $eV_a/h(\nu - \nu_0) \gg 1$

$$\frac{J}{J_v} = 1 + \frac{8}{5}\left(\frac{J_s}{J}\right)^{-1/4}\left(\frac{eV_a}{h(\nu-\nu_0)}\right)^{-1/2} + O\left(\frac{eV_a}{h(\nu-\nu_0)}\right)^{-3/4}. \tag{33}$$

For sufficiently large V_a this equation shows that $J = J_v$ for all values of $J_s > J$. For example if $eV_a/h(\nu - \nu_0) \geqslant 10^3$ then $J_v \leqslant J \leqslant 1{\cdot}05J_v$ for all $J_s \geqslant J_v$. Consequently if J_s is gradually increased from zero at constant, large V_a then J will be equal to J_s throughout the region $0 \leqslant J_s \leqslant J_v$, for which there is no space charge limitation, whereas in the region $J_v \leqslant J_s \leqslant \infty$ complete limitation abruptly sets in and $J = J_v$. At lower values of V_a it is necessary to resort to computation and figure 3 shows the dependence of J on V_a for prescribed values of J_s/J evaluated from table 1. The ordinate here is expressed in terms of the current density J_1 of equation (31), and the broken line represents the Langmuir–Child limit of equation (32). For a given V_a the close spacing of the curves, which represent a factor of 100 variation in J_s, shows the strong limiting effect of space charge on the anode current J. However the approach to complete space charge limitation is less abrupt the lower the anode voltage. All the curves lie above the Langmuir–Child limit and are tangent to it at sufficiently large values of V_a, as required by equation (33). Furthermore the various curves separate from this dotted line in the manner required by this equation, namely those for low values of the parameter J_s/J separate first, but it is evident from figure 3 that the curves change their order at lower values of V_a. This suggests that, for a given V_a, the current J is not a single valued function of J_s. Figure 4(*a*) demonstrates this fact more clearly by presenting J as a function of J_s for specified positive values of V_a. In all cases J/J_v exhibits a maximum that decreases in magnitude and moves towards lower values of

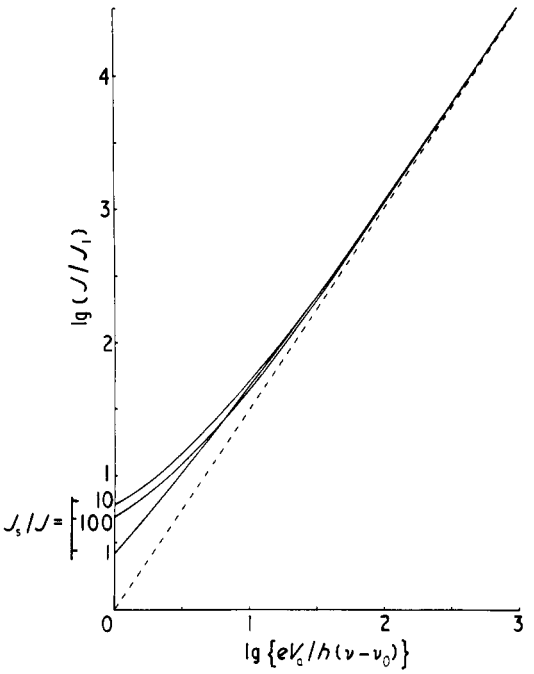

Figure 3. Anode current–voltage characteristics for various saturation currents. The broken line is the Langmuir–Child limit.

J_s/J_v with increase in V_a. However multiplication of these axes by J_v shows that the maximum in J increases and moves towards greater values of J_s with increase in V_a as physically expected. The ringed coordinates on these curves correspond to the onset of space charge limitation; the curve being defined by $J = J_s$ to the left of these coordinates. The broken lines represent the completely space charge limited current, attained as $J_s \to \infty$. This limit is given by the first term in the following power series that is valid for all $eV_a/h(\nu - \nu_0)$ and for $J_s/J \gg 1$

$$\frac{J}{J_v} = \left(1+\frac{h(\nu-\nu_0)}{eV_a}\right)^{3/2} + \frac{8}{5}\left(\frac{J_s}{J}\right)^{-1/4}\left(\frac{h(\nu-\nu_0)}{eV_a}\right)^{1/2}\left(1+\frac{h(\nu-\nu_0)}{eV_a}\right) + O\left(\frac{J_s}{J}\right)^{-1/2}. \tag{34}$$

The similarity between equations (33) and (34) arises because they are both approximations to the same general expression. Figure 4(*b*) shows the dependence of J on J_s for zero and negative values of V_a with the currents expressed in terms of J_1. In this case the maximum in J decreases as V_a is made more negative but the maximum always occurs for saturation currents of the order $J_s = 27J_1$. Once again the ringed coordinates indicate the onset of space charge limitation, as discussed in § 6, and the broken line represents the completely space charge limited current given by equation (34) which, for this purpose, can be rewritten as $J = J_1\{1 + eV_a/h(\nu-\nu_0)\}^{3/2}$. The information contained in figures 4(*a*) and 4(*b*) is shown collectively in figures 5(*a*) and 5(*b*) where the three curves of anode current depicted correspond to the onset of space charge limitation, the maximum current within the limited region and the completely space charge limited current. At sufficiently high values of V_a the maximum and onset curves combine above the complete limit indicating that the curves of J against J_s at constant

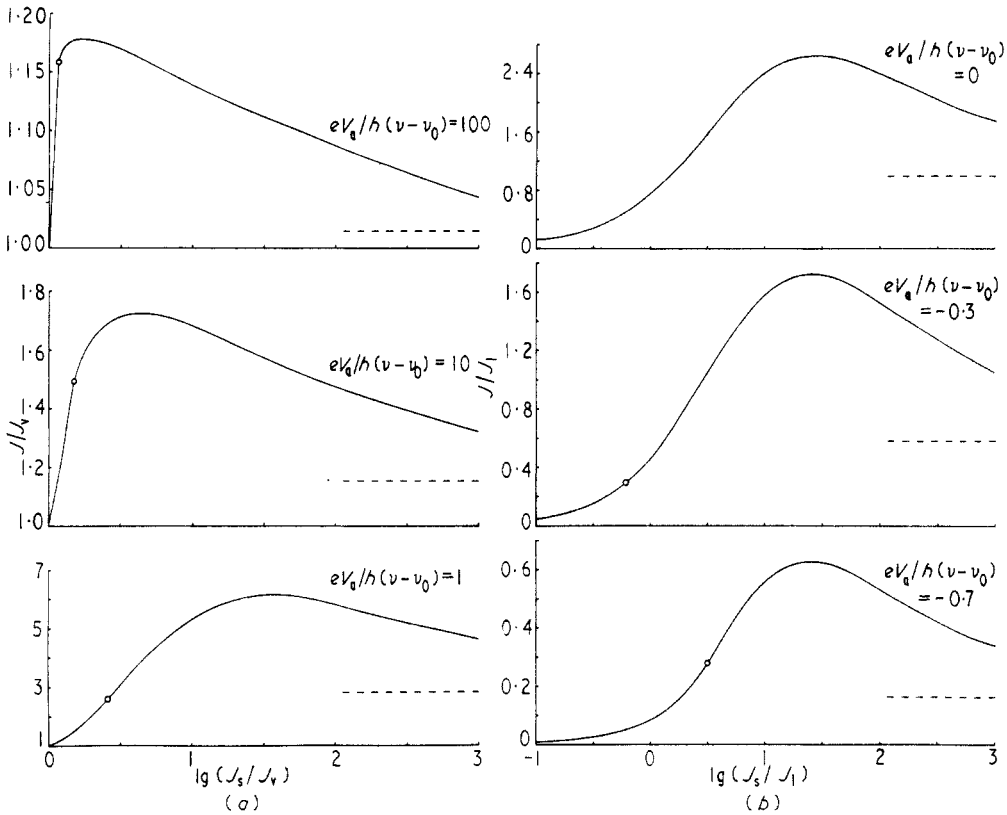

Figure 4. Dependence of anode current on saturation current for various anode voltages. The ringed coordinates correspond to the onset of space charge limitation and the broken lines represent the completely limited current. (*a*) Positive anode voltages, currents expressed in terms of J_v. (*b*) Negative anode voltages, currents expressed in terms of J_1.

V_a have a small negative slope throughout the limited region, in agreement with equation (33). For large positive and negative anode voltages the anode current for complete space charge limitation is less than that for the onset of limitation. However the situation is reversed for $eV_a/h(\nu-\nu_0)$ lying between $+1{\cdot}23$ and $-0{\cdot}50$.

8. The behaviour of the potential minimum

The magnitude V_m and position x_m of the potential minimum are most conveniently described in terms of the parameters $eV_m/h(\nu-\nu_0)$ and x_m/x_a. Equation (18) shows that $eV_m/h(\nu-\nu_0)$ is a simple function of J/J_s and it follows from equation (21) that x_m/x_a is a function of β only. However β is a single valued function of α which implies that x_m/x_a is a function of the two parameters J/J_s and $eV_a/h(\nu-\nu_0)$. Figures 6(*a*) and 6(*b*) shows x_m/x_a as a function of J_s/J for various specified values of anode voltage. The extreme left hand coordinates on these curves correspond to the ringed coordinates in figures 4(*a*) and 4(*b*) marking the onset of space charge limitation. In the case of negative anode voltages the minimum makes its appearance at the anode and moves progressively towards the cathode with increase in J_s/J. However for positive anode voltages

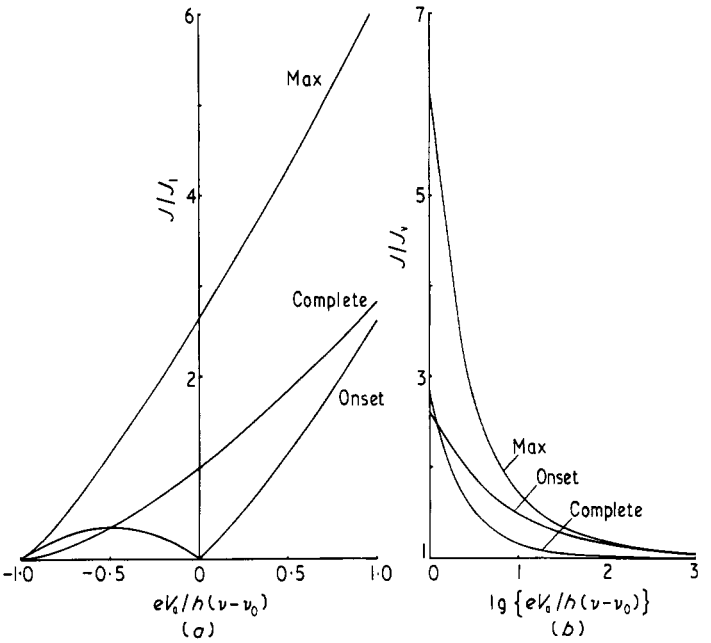

Figure 5. The anode current for onset of limitation, the maximum limited current and the completely limited current as functions of the anode voltage. (*a*) Small anode voltages, currents expressed in terms of J_1. (*b*) Large positive anode voltages, currents in terms of J_ν.

the minimum appears at the cathode, moves out a maximum distance from the cathode and then moves back to reach the cathode as $J_s/J \to \infty$. The maximum excursion from the cathode is always less than $0{\cdot}5x_a$, it decreases with increase of anode voltage and occurs very near $J_s/J = 4$, corresponding to $eV_m/h(\nu-\nu_0) = -0{\cdot}5$. Figure 7 shows the behaviour of this maximum in x_m/x_a as a function of positive anode voltage. The broken line here represents the following theoretical expression valid for very large anode voltages

$$\left(\frac{x_m}{x_a}\right)_{max} = 0{\cdot}590\left(\frac{eV_a}{h(\nu-\nu_0)}\right)^{-3/4}.$$

The situation occurring at zero anode voltage has been briefly discussed in relation to figure 2(*a*) where it corresponds to the singular point at which the curves for $x_m = x_a$ and $x_m = 0$ meet each other. Figure 6(*b*) which is based on an unambiguous treatment, shows that the minimum starts at $x_m/x_a = 0{\cdot}5$, corresponding to $J = J_s = 0$, and then moves towards the cathode as current flow takes place.

9. Discussion

It is essential that a vacuum photoelectric device designed for quantitative measurement of radiant energy should be operated under conditions such that no space charge limitation of the current takes place. Figure 2(*b*) gives the upper limit to the saturation current J_s that can be collected for a given V_a without such limitation and the corresponding maximum illumination of the cathode can be determined from this value.

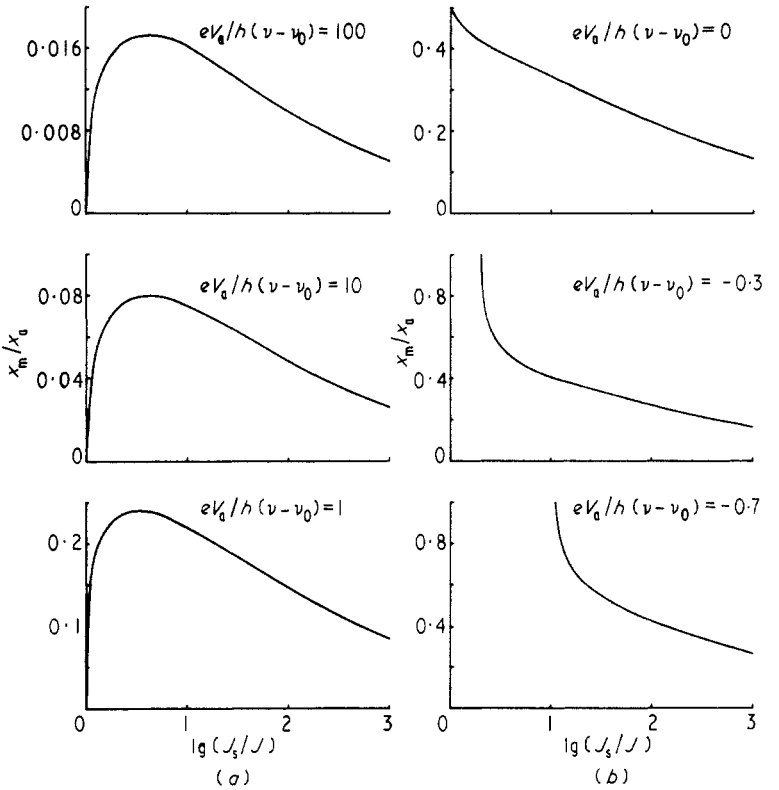

Figure 6. The position of the potential minimum as a function of the current ratio J_s/J for various anode voltages. (*a*) Positive anode voltages. (*b*) Negative anode voltages.

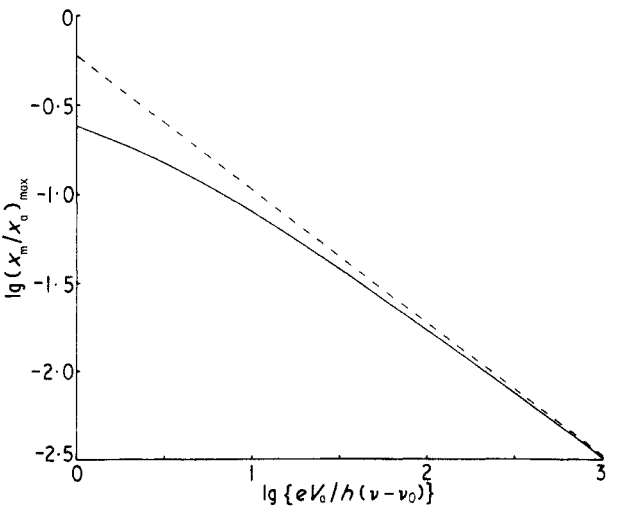

Figure 7. The maximum separation of the potential minimum from the cathode as a function of positive anode voltage. The broken curve represents the asymptotic expression.

However it cannot be inferred that limitation is not taking place if the anode current J is less than this critical value of J_s corresponding to the onset of limitation. Figure 5(*b*) shows that for $eV_a/h(\nu-\nu_0) > 1{\cdot}23$ the limited current can be less than this value of J_s, consequently a sufficient condition for absence of limitation is

$$J < J_{\text{complete}} = J_v\left(1+\frac{h(\nu-\nu_0)}{eV_a}\right)^{3/2}.$$

It follows from this expression that, as a general guide, no space charge limitation is possible if the saturation and anode currents are less than the Langmuir–Child limit. This conclusion is unaltered by the fact that the theoretical model overestimates the number of low energy photoelectrons, as discussed in § 5.

The negative quadrant in figure 2(*a*) has particular bearing on the validity of experiments that measure cathode work functions, Planck's constant or photoelectron energy distributions by the retarding potential technique. The form of this curve shows that it is impossible to prevent space charge limitation when collecting either just the very high energy electrons, $-eV_a/h(\nu-\nu_0) \simeq 1$, or when collecting almost the complete spectrum of electron energies, $-eV_a/h(\nu-\nu_0) \simeq 0$. Space charge limitation is likely to be more marked in this latter region since nearly the full saturation current is collected there. As an example of this situation consider the experimental arrangement used by Dubridge and Hergenrother (1933) consisting of a flat molybdenum cathode, $38 \times 2{\cdot}6\ \text{mm}^2$ and a parallel nickel anode 4·8 mm away. The range of cathode illuminating wavelengths had an average quantum energy situated above the molybdenum threshold by $h(\nu-\nu_0) = 0{\cdot}8$ eV. For these numerical values equation (31) gives $I_1 = 7{\cdot}1\ \mu\text{A}$. Reference to figure 2(*a*) shows that a saturation current of this magnitude would not permit the photoelectron energy spectrum to be examined over the lower $\frac{2}{5}$ of its range by the retarding potential technique. However at the time that these experiments were carried out, the available monochromatic sources of radiation would have produced currents many orders below this value and there is no reason to expect that the results obtained were influenced by space charge effects.

When operating at very low anode potentials the nature of the anode material must be taken into account since the potential to be used in these calculations is in fact the sum of the applied potential and the contact potential between the electrode metals. Therefore the curve of figure 4(*b*), corresponding to $V_a = 0$, gives the current that can flow between similar parallel electrodes in vacuum at the same applied potential when one of them is illuminated. In particular the curve shows that the maximum current density that can flow between the electrodes, spaced a distance x_a apart, is

$$J_{\max} = 2{\cdot}63J_1 = \frac{2{\cdot}63}{9\pi}\left(\frac{2e}{m}\right)^{1/2}\left(\frac{h(\nu-\nu_0)}{e}\right)^{3/2} x_a^{-2}.$$

Section 8 shows that the magnitude of the potential minimum V_m and its position x_m are independent quantities since the former parameter is not an explicit function of the anode voltage. Figure 8 illustrates this independence by presenting V_m and x_m as functions of J_s/J with variation in this latter parameter brought about by variation of either J_s or of J separately. In both cases it is assumed that $eV_a/h(\nu-\nu_0) \gg 1$ and also that the current is completely space charge limited, therefore $J = J_v$ at all times. The upper curve corresponds to variation of J_s at constant J achieved by varying the intensity of cathode illumination while maintaining the anode potential constant so that $J = J_v$.

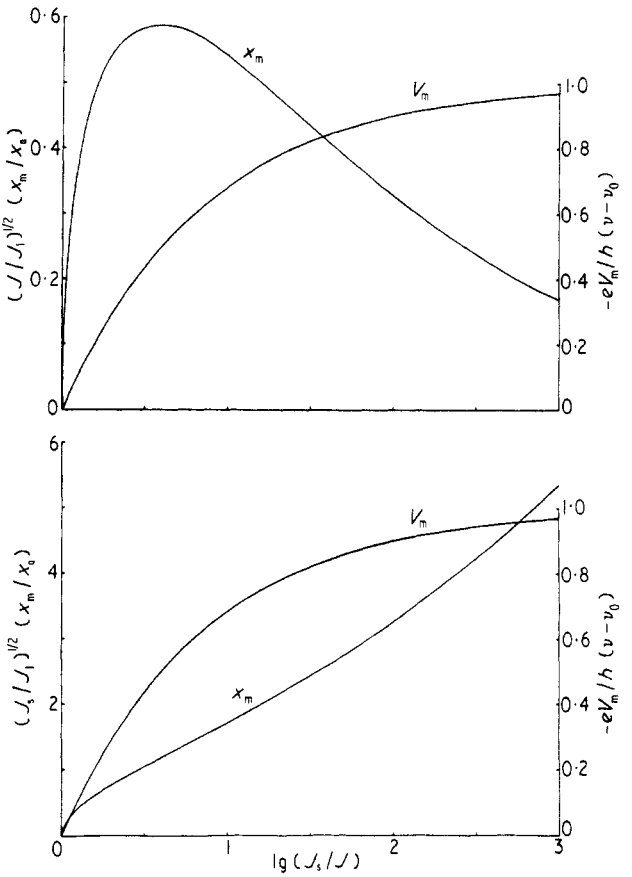

Figure 8. Dependence of the position of the potential minimum and its magnitude on the current ratio J_s/J for large positive anode voltages. The upper curves are for constant J and the lower curves for constant J_s.

In this case x_m exhibits the same behaviour as in figure 6(*a*) and the ordinate here is so chosen that the one curve is valid for all V_a. The lower curve corresponds to variation of J at constant J_s achieved by varying V_a, thereby varying $J = J_v$, and maintaining a constant cathode illumination. The ordinate here is chosen such that the one curve is valid for all J_s. In both cases the curves for V_m are identical whilst the behaviour of x_m is entirely different.

Appendix

Substitution of equation (13) into (9) and use of equations (4), (8), (10), (25) and (26) results in the equation

$$\frac{h^3}{32\sqrt{(2)}\pi^2 AIm^{3/2}(kT)^{5/2}}\left(\frac{dV}{dx}\right)^2 = I(\epsilon) \pm I(\epsilon, \delta) - I(\delta)$$

where

$$I(\epsilon) = \int_0^\infty y^{1/2} \ln\{1+\exp(\epsilon - y)\}\, dy$$

$$I(\epsilon, \delta) = \int_0^{\epsilon-\delta} y^{1/2} \ln\{1+\exp(\epsilon - y)\}\, dy$$

$$I(\delta) = \int_0^\infty y^{1/2} \ln\{1+\exp(\delta - y)\}\, dy.$$

In the case of the integral $I(\epsilon)$ change the variable to $z = \epsilon - y$ and divide the new range of integration, $-\infty$ to ϵ, into the two ranges 0 to ϵ, and $-\infty$ to 0.

$$I(\epsilon) = \int_0^\epsilon (\epsilon - z)^{1/2} \ln(1+\exp z)\, dz + \int_0^\infty (\epsilon + z)^{1/2} \ln(1+\exp -z)\, dz$$

where the variable has been changed in sign in the last integral. In the first integral above use $\ln(1+\exp z) = z + \ln(1+\exp -z)$. Absorb that part of the last integral lying between the limits of 0 and ϵ into the first integral to form the expression $(\epsilon - z)^{1/2} + (\epsilon + z)^{1/2}$ in the integrand. For this integral $0 \leqslant z \leqslant \epsilon$, so enabling a binomial expansion of the integrand. The result of these operations is

$$I(\epsilon) = \int_\epsilon^\infty (\epsilon + z)^{1/2} \ln(1+\exp -z)\, dz + \int_0^\epsilon (\epsilon - z)^{1/2} z\, dz$$
$$+ 2\epsilon^{1/2} \int_0^\epsilon \ln(1+\exp -z)\, dz - \tfrac{1}{4}\epsilon^{-3/2} \int_0^\epsilon z^2 \ln(1+\exp -z)\, dz$$
$$- \tfrac{5}{64}\epsilon^{-7/2} \int_0^\epsilon z^4 \ln(1+\exp -z)\, dz + \ldots .$$

Since z is a positive quantity in all these integrals the following expansion can be used

$$\ln(1+\exp -z) = \sum_{n=1}^{\infty} (-1)^{n+1} n^{-1} \exp(-nz).$$

The resulting integrals containing integral powers of z can be performed through successive integration by parts.

$$I(\epsilon) = \sum (-1)^{n+1} n^{-1} \int_\epsilon^\infty (\epsilon + z)^{1/2} \exp(-nz) dz + \tfrac{4}{15}\epsilon^{5/2} + 2\epsilon^{1/2} \sum (-1)^{n+1} n^{-2}$$
$$\times \{1 - \exp(-n\epsilon)\} - \tfrac{1}{4}\epsilon^{-3/2} \sum (-1)^{n+1} n^{-4}$$
$$\times \{2 - (n^2\epsilon^2 + 2n\epsilon + 2)\exp(-n\epsilon)\} - \tfrac{5}{64}\epsilon^{-7/2} \sum (-1)^{n+1} n^{-6}$$
$$\times \{24 - (n^4\epsilon^4 - 4n^3\epsilon^3 + 12n^2\epsilon^2 + 24n\epsilon + 24)\exp(-n\epsilon)\} + \ldots .$$

The summations over the independent terms can be evaluated in terms of Bernoulli numbers. However the remaining integral cannot be performed analytically but it can be bracketed between two closely spaced limits as follows. Within the range of integration the factor $(\epsilon + z)^{1/2}$ lies between $(2\epsilon)^{1/2}$ and $(\epsilon + z)(2\epsilon)^{-1/2}$ and it readily follows that the complete integral lies between $(2\epsilon)^{1/2} \Sigma (-1)^{n+1} n^{-2} \exp(-n\epsilon)$ and

$(2\epsilon)^{1/2}\sum(-1)^{n+1}n^{-2}(1+1/2n\epsilon)\exp(-n\epsilon)$. Finally if all powers of ϵ up to $\epsilon^{-7/2}$ are retained and also the dominant $n = 1$ exponential term then

$$I(\epsilon) = \frac{4}{15}\epsilon^{5/2} + \frac{\pi^2}{6}\epsilon^{1/2} - \frac{7\pi^4}{1440}\epsilon^{-3/2} + O(\epsilon^{-7/2}, \epsilon^{1/2}\exp -\epsilon).$$

In the case of the integral $I(\epsilon, \delta)$ the index of the exponential is always positive and the logarithmic term can be expanded as follows

$$\ln\{1+\exp(\epsilon - y)\} = \epsilon - y + \sum(-1)^{n+1}n^{-1}\exp\{-n(\epsilon - y)\}$$

and this leads to

$$I(\epsilon, \delta) = \tfrac{2}{15}(\epsilon-\delta)^{3/2}(2\epsilon+3\delta) + \sum(-1)^{n+1}n^{-1}\exp(-n\epsilon)\int_0^{\epsilon-\delta} y^{1/2}\exp(ny)\,dy.$$

The integral here is analogous to one of the integrals contained in $I(\epsilon)$ in that it can be bracketed between two closely spaced limits. Within the range of integration the factor $y^{1/2}$ lies between $y(\epsilon-\delta)^{-1/2}$ and $(\epsilon-\delta)^{1/2}$ and it readily follows that the complete integral lies between

$$(\epsilon-\delta)^{1/2}\sum(-1)^{n+1}n^{-2}\left(\exp(-n\delta) - \frac{\exp(-n\delta)-\exp(-n\epsilon)}{n(\epsilon-\delta)}\right)$$

and

$$(\epsilon-\delta)^{1/2}\sum(-1)^{n+1}n^{-2}\{\exp(-n\delta)-\exp(-n\epsilon)\}.$$

Finally if all terms up to the dominant $n = 1$ term of the exponential are retained then

$$I(\epsilon, \delta) = \tfrac{2}{15}(\epsilon-\delta)^{3/2}(2\epsilon+3\delta) + O[(\epsilon-\delta)^{1/2}\{\exp(-\delta)-\exp(-\epsilon)\}].$$

The remaining integral $I(\delta)$ reduces to the same power series as that for $I(\epsilon)$ except that ϵ is replaced by δ.

References

Child C D 1911 *Phys. Rev.* **32** 492–511
Dubridge L A 1933 *Phys. Rev.* **43** 727–41
Dubridge L A and Hergenrother R C 1933 *Phys. Rev.* **44** 861–5
Fowler R H 1931 *Phys. Rev.* **38** 45–56
Fry T C 1921 *Phys. Rev.* **17** 441–52
Langmuir I 1913 *Phys. Rev.* **2** 450–86
—— 1923 *Phys. Rev.* **21** 419–35